Interplay between periodicity and nonlinearity of indirect excitons in coupled quantum wells

T. F. Xu[1], X. L. Jing[1], H. G. Luo[2,3], W. C. Wu[4], and C. S. Liu[1,4]

[1]*Department of Physics, Yanshan University, Qinhuangdao 066004, China*
[2]*Center for Interdisciplinary Studies and Key Laboratory for Magnetism and Magnetic Materials of the Ministry of Education, Lanzhou University, Lanzhou 730000, China*
[3]*Beijing Computational Science Research Center, Beijing 100084, China*
[4]*Department of Physics, National Taiwan Normal University, Taipei 11677, Taiwan*
(Dated: February 24, 2013)

Inspired by a recent experiment of localization-delocalization transition (LDT) of indirect excitons in lateral electrostatic lattices [M. Remeika *et al.*, Phys. Rev. Lett. **102**, 186803 (2009)], we investigate the interplay between periodic potential and nonlinear interactions of indirect excitons in coupled quantum wells. It is shown that the model involving both attractive two-body and repulsive three-body interactions can lead to a natural account for the LDT of excitons across the lattice when reducing lattice amplitude or increasing particle density. In addition, the observations that the smooth component of the photoluminescent energy increases with increasing exciton density and exciton interaction energy is close to the lattice amplitude at the transition are also qualitatively explained. Our model provides an alternative way for understanding the underlying physics of the exciton dynamics in lattice potential wells.

I. INTRODUCTION

Indirect excitons (spatially separated electron-hole pairs) in coupled quantum wells (CQWs) can have a long lifetime and a high cooling rate. With these two merits, Butov *et al.* have successfully cooled the trapped excitons to the order of 1K and have observed surprisedly that excitons form two, inner and external, rings to which periodic bright spots appear in the external ring.[1,2] Although there is no clear evidence that these excitons are condensed into the BEC state, it is fascinating enough to see some puzzling particle number distributions in various confined potential wells.[3,4] More recently, periodic potential (lattices) due to gate voltages was created for indirect excitons of built-in electric dipole moment. It enables observation of localization-delocalization transition (LDT) for transport across the lattice with reducing lattice amplitude or increasing particle density.[5] This gives an opportunity to understand further the complex dynamical behaviors of indirect excitons.

In the literature, a charge separated transportation mechanism was proposed,[6] which gave a satisfactory explanation to the formation of exciton rings and the dark region between the inner and the external rings. However the origin of the periodic bright spots in the external ring can not be fully understood within the above framework. Alternatively a self-trapped interaction model involving attractive two-body and repulsive three-body interactions in the system was proposed.[7,8] It was shown that the interplay between the two-body attraction and the three-body repulsion can give a good account to the periodic bright spots in the external ring. In addition, the self-trapped interaction model also explained well the abnormal exciton distribution in an impurity potential, where the photoluminescence (PL) pattern becomes much more compact than a Gaussian with a central intensity dip, exhibiting an annular shape with a darker central region.[3] Moreover, the model also captured some other experimental details, for instances, the dip can turn into a tip at the center of the annular cloud when the sample is excited by higher power lasers.

The success of the self-trapped interaction model in understanding various phenomena has motivated us to investigate the LDT phenomenon reported in Ref. [5] using the same model. It will be shown that the complex LDT as well as other dynamic behaviors can also be qualitatively explained by the self-trapped interaction model.

This paper is organized as follows. In Sec. II, we introduce the self-trapped interaction model described by a phenomenological nonlinear Schrödinger equation. An important factor regarding how the exciton distribution depends on temperatures and energies is detailed. In Sec. III, numerical calculations and detailed discussions are given for studying the LDT of transports across the lattice. It will be shown that the model introduced in Sec. II can lead to a reasonably good explanation for LDT. Sec. IV is a brief summary.

II. MODEL

The idea of the self-trapping model came from the density dependence of various observed PL spectroscopy.[2–5] As a matter of fact, intensity of PL spectroscopy is proportional to the exciton number density and therefore complex experimental PL data will reveal complex interaction between excitons. It is clear that the interaction between excitons is neither purely attractive, nor purely repulsive. If it is purely repulsive, it could drive the system towards homogeneous distribution. On the contrary,

if it's purely attractive, the system will become unstable and eventually collapse when the exciton density is larger than some critical value. Thus it is reasonable to speculate that at low densities the interaction is dominated by an attraction, while at high densities a repulsion must exist to prevent the system against collapses.[7] The observation that exciton cloud first contracts then expands by increasing the excitation power gives a strong support to the above scenario.[3]

Excitons behave as electric dipoles, so strong Coulomb repulsion will govern the indirect excitons in CQWs at high densities to which dipoles are aligned in parallel.[9] However at low densities such that two dipoles change from aligning in parallel to inclined, the attraction between the electron of one exciton and the hole of the other exciton will dominate instead.[10] In addition to Coulomb interactions, exchange effect may be another important factor for interactions. When two excitons approach to each other, exchange interaction between two electrons (or two holes) will become more important. This may be another source of the attraction between excitons.

In the dilute limit, it is assumed that indirect excitons in CQWs are governed by two-body attractions and three-body repulsions. Equivalently one can consider the following scaled *nonlinear* Schrödinger equation[7,8]

$$-\frac{1}{2}\nabla^2\psi_j(\mathbf{r}) + [V_{\mathrm{ex}}(\mathbf{r}) - g_1 n + g_2 n^2]\psi_j(\mathbf{r}) = E_j\psi_j(\mathbf{r}), \quad (1)$$

where $\psi_j(\mathbf{r})$ and E_j are the j-th energy eigenfunction and eigenvalue and V_{ex} denotes the external potential. The eigenfunction is normalized under $\int_\Omega |\psi_j(\mathbf{r})|^2 d\Omega = 1$. In Eq. (1), all lengths and energies are scaled in units of σ_{PL} and $\hbar^2/m^*\sigma_{\mathrm{PL}}^2$ respectively, where $m^* = m_e/2$ is effective mass of the exciton and σ_{PL} is the root-mean-square radius of the exciton cloud observed via PL.[8] Considering the special property of the system, local probability density of excitons $[n = n(\mathbf{r})]$ will be taken to be

$$n(\mathbf{r}) = \sum_{j=1}^{\mathcal{N}} \eta(E_j)|\psi_j(\mathbf{r})|^2, \quad (2)$$

where $\mathcal{N}$ denotes the total number of bound states involved and $\eta(E_j)$ is the probability (or distribution) function for energy-level E_j that satisfies the normalization condition $\sum_{j=1}^{\mathcal{N}} \eta(E_j) = 1$. At the mean-field level, two- and three-body coupling constants, g_1 and g_2, are defined positively, which will be proportional to N and N^2 with N being the number of excitons. Note that exciton number density can be controlled by and proportional to the excitation laser power P, thus g_1 is proportional to P in the current model.

Determination of the distribution function $\eta(E_j)$ in (2) requires considering both complex *energy relaxation* and *recombination* processes. At low exciton densities ($n \ll 1/a_B^2$, a_B being Bohr radius), relaxation due to exciton-exciton and exciton-carrier scattering can be neglected[11] and consequently relaxation time is dominated by the scattering of excitons with acoustic phonons. At low bath
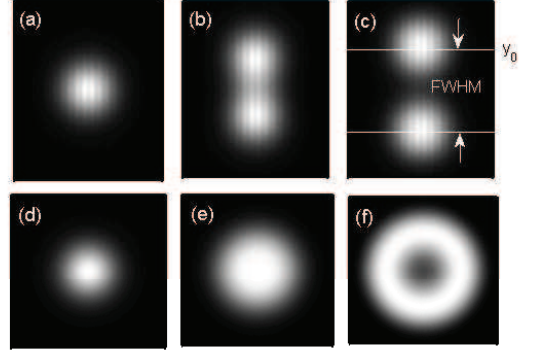

FIG. 1. Calculated spatial probability density distribution of highly degenerate indirect excitons, $n(x,y)$, for low densities ($g_1 = 10$) [frame (a) & (d)], intermediate densities ($g_1 = 20$) [frame (b) & (e)], and high densities ($g_1 = 30$) [frame (c) & (f)]. Frame (a)-(c) are with a lattice potential $V_{\mathrm{ex}} = v_0 \cos(2\pi x/\lambda)$ ($v_0 = 50$ and $\lambda = 0.05$), while (d)-(f) are without a lattice potential ($v_0 = 0$). In all frames, $g_2 \equiv 0.001 g_1^2$, α is fixed at 0.1, and x and y axes are in units of σ_{PL} (see text). The results are intended to be compared to those in Fig. 1 of Ref. 5. In frame (c), FWHM (calculated in Fig. 3) and y_0 (used in Fig. 2) are denoted.

temperatures, ($T_b < 1$ K), this kind of relaxation rate decreases dramatically due to the low phonon density.[12] For the recombination process, on the other hand, because excitons in the lowest self-trapped level are quantum degenerate, they are dominated by the stimulated scattering when the occupation number is more than a critical value. Strong enhancement of the exciton scattering rate has been observed in the resonantly excited time-resolved PL experiment.[13] Therefore, even though the phonon scattering rate is larger than the radiative recombination rate, it is in reality that the system does not reach thermal equilibrium. Following Ref. [8], in accord with the discrete PL spectroscopy reported in Ref. [14], $\eta(E_j)$ will have the following form

$$\eta(E_j) = C \exp[\alpha(E_j - \mu)], \quad (3)$$

where C is the normalization factor, μ is the chemical potential, and α can be viewed as an "effective temperature".

III. RESULTS AND DISCUSSIONS

A. Spatial exciton distributions with or without lattices

Key features of indirect excitons with or without lattices, as reported in Ref. [5], are the following. LDT for transport across the lattice was observed with reducing lattice amplitude or increasing exciton density. The inner ring, which was observed in the PL patterns of indirect excitons without lattices, persists in the lattice

case. For relatively low excitation power ($P = 3.7\ \mu$W), outer ring effect does not emerge because of low particle number density and hence low drift and diffusion of electrons and holes. However, for relatively higher excitation power ($P = 12\ \mu$W), in addition to the inner ring, outer ring seems to exist in the case without the lattices (see Fig. 1.(i) of Ref. [5]). With the lattices (see Fig. 1.(f) of Ref. [5]), outer ring transforms to spatially separated clouds, while inner ring persists.

Based on the above observations, in the current localized-delocalized system it seems that there are two kinds of excitons, whose spatial distributions could be governed by different mechanisms. The ones associated with the inner ring effect are ascribed to the *hot* excitons which have been studied in great details in Refs.[2,5,6,15]. The other ones are ascribed to the *cool* excitons whose formation and pattern are considered to be due to quantum degeneracy.[7,8].

When excitation power P is low, densities of both hot and cool excitons are low. They are all localized within the range of the laser spot (i.e., localization). When P is increased, densities of both kinds of excitons will increase for which inner ring forms due to transportation and cooling of the hot excitons. While cool excitons will form patterns due to quantum degeneracy arising from complex interactions. Delocalization effect increases with increasing the laser power P, to which radius of the inner ring as well as the distance between the two separated degenerate exciton clouds increase. As a matter of fact, full width at half maximum (FWHM) of the exciton cloud will change with the particle number density or the lattice potential amplitude, as shown in Fig. 3 of Ref. 5.

Here we shall focus on the LDT associated with highly degenerate low-energy (cool) excitons only. Spatial distributions of low-energy exciton density are calculated self-consistently based on Eqs. (1)–(3). The results are shown in Figs. 1(a)–1(c) for the case of a periodic lattice potential, $V_{\rm ex} = v_0 \cos(2\pi x/\lambda)$ with $v_0 = 120$ and $\lambda = 0.05$, and in Figs. 1(d)–1(f) for the case without a lattice potential ($v_0 = 0$). In the case with lattice potential, a weak rectangular potential well is applied to ensure the strip pattern along the lattices (*i.e.*, with the Dirichlet boundary condition). In our model, highly degenerate excitons are self-trapped due to competition between complex interactions and the nonequilibrium energy distribution. Apart from the periodic lattice potential, any additional weak external potential will only have minor effect on the results. In our calculations, the wave function is chosen to be a Gaussian initially. All self-trapped energy eigenstates ψ_j with $\varepsilon_j < 0$ are solved and will contribute to the spatial distribution.

As mentioned before, at low excitation powers P low-energy exciton density profile essentially coincides with the excitation laser spot. In our model, this arises due to the dominant attraction between excitons in the dilute limit and at the same time only ground state contributes to the self-trapping. The ground-state wave function is s-wave with a maximum at the center [see Figs. 1(a) and
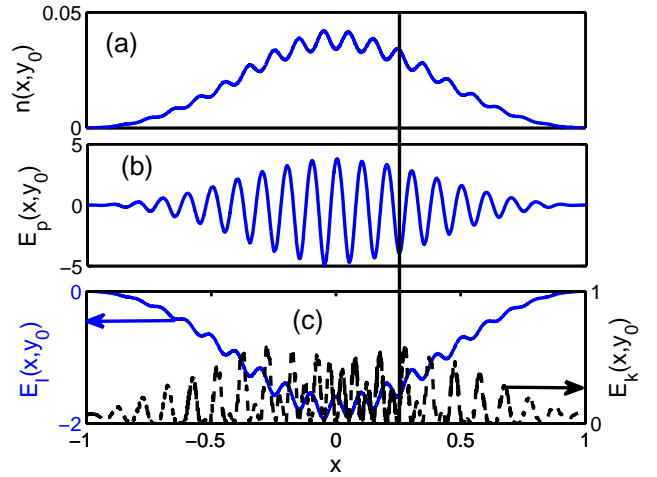

FIG. 2. (Color online) (a) Exciton probability density distribution $n(x, y_0)$ with y_0 denoted in Fig. 1(c). (b) Lattice potential energy density $E_p(x, y_0) \equiv V_{\rm ex}(x)n(x, y_0)$ plotted vs. x. (c) Spatially dependent interaction energy density $E_I(x, y_0)$ and kinetic energy density $E_k(x, y_0)$ plotted vs. x. Parameters used are the same as those in Fig. 1(c), except a larger $g_1 = 50$ and $v_0 = 100$ to account for the experiment. Vertical line shows that maxima in density $n(x, y_0)$ correspond to minima in periodic potential energy density $E_p(x, y_0)$. In all frames, x axis is in units of $\sigma_{\rm PL}$. The results are intended to be compared to those in Fig. 2 of Ref. 5.

1(d)]. Excitons are localized and do not travel beyond the excitation spot.

When exciton number is increased with higher excitation power P, excitons can delocalize and spread beyond the excitation spot [see Figs. 1(b), 1(c), 1(e), and (1f)]. In these cases, effect of repulsion becomes more important which results more energy eigenstates involved in the self-trapping. The first excited states are nearly twofold degenerate p-wave with a node at the center. Superposition of the ground-state s-wave and the two first-excited-state p-wave wavefunctions leads to an annular distribution with a hole at the center in the case without lattices [see Fig. 1(f)]. With the lattices, two-fold degeneracy is lifted and consequently ring-shaped delocalized excitons shift to two separate clouds at high excitation powers [see Fig. 1(c)].

B. Spatially dependent PL energy

A PL image of indirect excitons in the delocalized regime, plotted as energy vs. space, is presented in Fig. 2(a) of Ref. 5. As a matter of fact, both integrated PL intensity $I(x)$ and the average PL energy $\hbar\omega(x)$ show a small modulation at the lattice period superimposed on a smoothly varying profile. In particular, the average PL energy shows a dome carve shape.

In fact in CQWs, spatially dependent energy of indi-

rect excitons, which is directly related to the PL energy $\hbar\omega$, involves four major contributions. The first part is the intrinsic energy that includes contributions due to the band gap, the Coulomb interaction between electrons and holes, and the electric potential used to form indirect excitons. Intrinsic energy of exciton mainly contributes to the smooth part of the PL energy $\hbar\omega$ since it does not change with positions when experimental condition remains unchanged. The second part is the kinetic energy E_k. Near the laser spot, excitons are hot with a large kinetic energy. It is believed that this is the main cause why a high energy distribution is located in the center regime. The third part is the interaction energy E_I. It also contributes to the smooth part of the PL energy $\hbar\omega$. Within our model, when exciton interaction is in the repulsion-dominant regime, E_I increases with the exciton density n and thus smooth part of $\hbar\omega$ will increase with increasing the excitation power P. Moreover, reducing the cloud size corresponds to increasing the exciton density when excitation power P remains unchanged. Therefore smooth part of $\hbar\omega$ will increase with reducing the cloud size. The last part is the lattice potential energy E_p. Within the Thomas-Fermi approximation, it is easy to verify that E_p dominates over E_I and E_k in such a dilute system (see later). This is why maxima in exciton number density (and equivalently the PL intensity) correspond to minima in the periodic potential energy density E_p (see Fig. 2).

Within the same model, average energy density and number distribution of highly degenerate excitons are calculated and shown in Fig. 2. These are intended to be compared to those reported in Fig. 2 of Ref. 5. Apart from the smooth part mainly due to the intrinsic energy, spatially dependent kinetic energy density of degenerate excitons can be calculated via[8]

$$E_k(\mathbf{r}) = \sum_{j=1}^{\mathcal{N}} \left[\eta(E_j) \left(\left| \frac{\partial \psi_j(\mathbf{r})}{\partial x} \right|^2 + \left| \frac{\partial \psi_j(\mathbf{r})}{\partial y} \right|^2 \right) \right], \quad (4)$$

while the interaction (mean-field) energy density is given by $E_I(\mathbf{r}) = -g_1 n(\mathbf{r})^2 + g_2 n(\mathbf{r})^3$ and the lattice potential energy density is given by $E_p(\mathbf{r}) = V_{\text{ex}}(\mathbf{r})n(\mathbf{r})$, which are obtained by multiplying $\eta(E_j)\psi_j^*(\mathbf{r})$ to Eq. (1) and summing over j.

Fig. 2(a) shows the calculated spatial probability density distribution of degenerate excitons, $n(x, y_0)$. Here y_0 corresponds to center of the upper cloud in y direction [see Fig. 1(c)]. The spatial lattice potential energy density $E_p(x, y_0)$, kinetic energy density $E_k(x, y_0)$, and interaction energy density $E_I(x, y_0)$ are presented in Figs. 2(b) and 2(c) respectively. In view of Fig. 2, E_k and E_I are about one order of magnitude smaller than E_p. This means that Thomas-Fermi approximation is valid in such a dilute exciton system. Consequently exciton number distribution is mainly determined by the periodic potential energy E_p. The higher the E_p is, the larger the local PL energy is. On the contrary, the lower the E_p is, the higher the local exciton number density is.
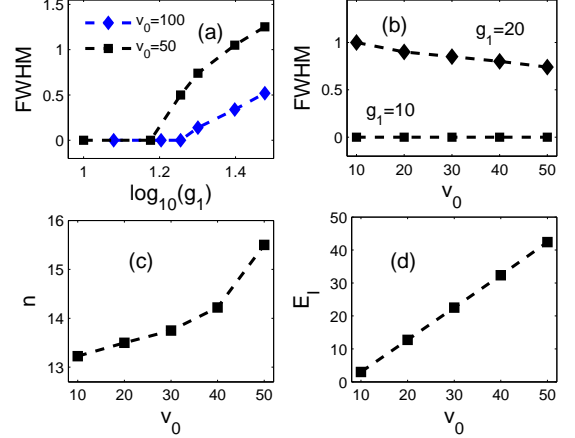

FIG. 3. (Color online) Calculated FWHM of delocalized exciton clouds vs. (a) $\log_{10}(g_1)$ ($g_1 \propto$ exciton number density n) for lattice amplitude $v_0 = 50$ and 100 and (b) v_0 for different n with $g_1 = 10$ and 20. (c) Calculated number density n at the LDT point as a function of lattice amplitude v_0. (d) Calculated interaction energy density $E_I(0, y_0)$ at the LDT point as a function of lattice amplitude v_0. $(0, y_0)$ corresponds to the outer cloud center. The results are intended to be compared to Fig. 3 in Ref. 5.

As PL intensity is proportional to the local exciton number density, it results that minima in energy correspond to the maxima in intensity. Equivalently the largest exciton number density (and hence the PL intensity) are located in the bottom of the periodic potential energy.

C. Interplay between periodic potential and nonlinear interaction

In view of the results shown in Figs. 3(a) and 3(b) of Ref. [5], it is surprising to see that FWHM of the exciton cloud (across the lattice) decreases with increasing the lattice amplitude. On the contrary, the excitation power needed for the transition from localized to delocalized regimes increases with the increase of the lattice amplitudes [see Figs. 3(c) of Ref. 5]. This is likely due to the reduction of the particle tunneling rate across the lattice. Thus a large laser power is needed to obtain exciton delocalized distribution when increasing the lattice amplitude.

Fig. 3 studies the effects of number density and lattice amplitude on LDT of degenerate excitons. Here, as the dynamics of outer cloud is focused on, we define FWHM as the distance (the extension) between centers of the two clouds along the y-direction [see Fig. 1(c)]. In Figs. 3(a) and 3(b), we show FWHM as a function of the particle number density (via changing g_1) and the lattice potential amplitude respectively. For weak excitation power P and low exciton number correspondingly, within our model both the attractive and repulsive interactions between excitons are weak. All particles are sitting in the

ground state and self-trapped in the shallow mean-field potential well. In this case, FWHM of exciton cloud is equal to zero and remains unchanged in the lower excitation power regime [see Fig. 3(a) and Fig. 3(b) with $g_1=10$]. When the excitation power P or the particle density n is increased to above some critical point, LDT occurs. Within our model, repulsive interaction dominates and consequently excitons will be sitting in both ground state and two-fold degenerate first-excited states. Due to the one-dimensional lattice potential, two-fold degeneracy of excited states is lifted and consequently two separated delocalized exciton clouds form.

In Fig. 3(c), we show the critical number density n for LDT as a function of lattice amplitude v_0. When v_0 is increased, before the LDT transition excitons are strongly localized in a single well center, while particle tunneling rate across the well is largely decreased. As a consequence, critical number density for LDT increases. Within our model, before the LDT transition a larger lattice amplitude v_0 corresponds effectively (or relatively) to a smaller exciton density. This also means that the effect of the repulsion is decreased while the effect of the attraction is increased. This explains why a blue-shift of the LDT is observed in the experiment. It gives another evidence to support our model.

In the delocalized regime, when excitation power P is low, only intrinsic energy and potential energy contribute to the exciton PL energy because interaction energy E_I is immaterial. When P is increases, however, E_I will become more important and contribute much more to the PL energy. Therefore, $\hbar\Delta\omega$, defined as the difference between $\hbar\omega$ and that associated with the lowest P for LDT, is dominated by E_I. Within our model, in the delocalized repulsion-dominant regime, interaction energy density E_I will increase monotonically with increasing the lattice amplitude v_0. Fig. 3(d) shows the calculated interaction energy density $E_I(0, y_0)$ at the LDT point as a function of lattice amplitude v_0. Here $(x, y) = (0, y_0)$ corresponds to the center of the outer cloud. In agreement with the experiment, it is seen that E_I at the LDT point is close to the value of the lattice amplitude v_0. This agreement gives a strong support that the scaled parameters used in the current context are reasonable.

IV. SUMMARY

In summary, we have investigated the interplay between periodic potential and nonlinear interaction of indirect excitons in coupled quantum wells, with or without a lattice potential. The model which takes into account the competition between a two-body attraction and a three-body repulsion along with a reasonable nonequilibrium energy distribution gives an alternative qualitatively good account on the localization-delocalization transitions (LDT) of excitons across the lattice when increasing the particle density or reducing the lattice amplitude.

[1] L. V. Butov, C. W. Lai, A. L. Ivanov, A. C. Gossard, and D. S. Chemla, Nature **417**, 47 (May 2002)

[2] L. V. Butov, A. C. Gossard, and D. S. Chemla, Nature **418**, 751 (2002)

[3] C. W. Lai, J. Zoch, A. C. Gossard, and D. S. Chemla, Science **303**, 503 (2004)

[4] A. T. Hammack, M. Griswold, L. V. Butov, L. E. Smallwood, A. L. Ivanov, and A. C. Gossard, Phys. Rev. Lett. **96**, 227402 (2006)

[5] M. Remeika, J. C. Graves, A. T. Hammack, A. D. Meyertholen, M. M. Fogler, L. V. Butov, M. Hanson, and A. C. Gossard, Phys. Rev. Lett. **102**, 186803 (2009)

[6] L. V. Butov, L. S. Levitov, A. V. Mintsev, B. D. Simons, A. C. Gossard, and D. S. Chemla, Phys. Rev. Lett. **92**, 117404 (2004)

[7] C. S. Liu, H. G. Luo, and W. C. Wu, J. Phys.: Condens. Matter **18** (2006)

[8] C. S. Liu, H. G. Luo, and W. C. Wu, Phys. Rev. B **80**, 125317 (2009)

[9] L. V. Butov, A. A. Shashkin, V. T. Dolgopolov, K. L. Campman, and A. C. Gossard, Phys. Rev. B **60**, 8753 (1990)

[10] V. I. Sugakov, Phys. Rev. B **76**, 115303 (2007)

[11] C. Piermarocchi, F. Tassone, V. Savona, , A. Quattropani, and P. Schwendimann, Phys. Rev. B **53**, 15834 (1996)

[12] H. Benisty, C. M. Sotomayor-Torrès, and C. Weisbuch, Phys. Rev. B **44**, 10945 (1991)

[13] L. V. Butov, A. L. Ivanov, A. Imamoglu, P. B. Littlewood, A. A. Shashkin, V. T. Dolgopolov, K. L. Campman, and A. C. Gossard, Phys. Rev. Lett. **86**, 5608 (2001)

[14] A. High, A. Hammack, L. Butov, L. Mouchliadis, A. Ivanov, M. Hanson, and A. Gossard, Nano Lett. **9**, 2094 (2009)

[15] R. Rapaport, G. Chen, D. Snoke, S. H. Simon, L. Pfeiffer, K. West, Y. Liu, and S. Denev, Phys. Rev. Lett. **92**, 117405 (2004)